Modern Physics Letters B, Vol. 17, Nos. 27 & 28 (2003) 1461–1476


World Scientific
www.worldscientific.com

# CHARACTERISTIC WAVEFUNCTIONS OF ONE-DIMENSIONAL PERIODIC, QUASIPERIODIC AND RANDOM LATTICES

X. Q. HUANG*,†, S. S. JIANG*, R. W. PENG*, Y. M. LIU*, F. QIU* and A. HU*

*National Laboratory of Solid State Microstructures and Department of Physics, Nanjing University, Nanjing 210093, China

†Institute of Communications Engineering, PLAUST, Nanjing 210016, China

Received 2 May 2003

We obtain analytically a universal expression of the resonant energies for any one-dimensional (1D) models with the defects having symmetric internal structures. In a 1D periodic system with the on-site energy $\varepsilon_0 = 0$ and a nearest-neighbor matrix element $t_0 = 1.0$, two classes of the most interesting and simplest wavefunction behaviors are numerically obtained for the resonant energies around (a) $0, \pm 1$, (b) $\pm(\sqrt{5}-1)/2, \sqrt{2}$, $\pm\sqrt{3}$, respectively. We show that similar wavefunction behaviors can be found widely in many quasiperiodic and random systems where the delocalization phenomena are predicted. We suggest that the envelope of these wavefunctions can be generally used as a criterion of delocalization of electronic states in 1D random and quasiperiodic lattices.

*Keywords*: Wavefunctions; quasiperiodic; random; delocalization.

PACS Number(s): 72.15.Rn, 71.23.An, 71.23.Ft

## 1. Introduction

In the past few years, extended electron states have been widely found in one-dimensional (1D) quasiperiodic and disordered systems.[1–31] For the quasiperiodic cases, Kumar *et al.* have found extended states in the Fibonacci sequence.[1] Numerous successive studies have shown that extended electronic states can be found in various aperiodic systems, such as the "mixed" Fibonacci sequence,[2–5] the generalized Fibonacci sequences,[6–9] and the Thue–Morse sequence.[10–13] For the random cases, Dunlap *et al.*[15] introduced the so-called random dimer model (RDM) and extended electron states have been found in this system.[16–18] In addition, some periodic-like extended electronic wavefunctions have been found numerically by Huang *et al.* in the model.[25] Later, Hilke *et al.* theoretically verified and improved these results by using the transfer matrix method.[26] More recently, we have numerically observed some periodic-like electronic wavefunctions in the disordered chains with the trimer-like impurities.[30]

The basic reason for the appearance of extended states in these systems has been traced to the existence of a certain type of short range correlation among the defects. It was shown analytically that at some special energy values, the

total transfer matrix for a defect offers an identity contribution to the full transfer matrix, so that at these energies the full disordered lattice effectively behaves as an ordered chain. In a later work, Wu *et al.* found a relationship between reflection coefficient and the total transfer matrix of a defect in the studied systems.[19] By using their expression they have successfully determined the resonant energies for several random models. Recently, this method has been applied to investigate the localization properties of some newly suggested random systems.[27,30] In fact, these studies with this technique are confined to one particular aspect — that the defects must have symmetric internal structures (SIS). In a recent paper, we have introduced the internal symmetric into a Fibonacci dielectric multilayer and found many perfect transmission peaks in the optical transmission spectra.[32,33] In this paper, we will show that the total transfer matrices of any symmetric defects are antisymmetric and demonstrate that the resonant energies of the random and quasiperiodic systems with the symmetric defects can be uniquely determined by the host parameters $\varepsilon_a$, $t_a$ and two matrix elements of the total transfer matrices. This newly developed method proves to be useful in determining the resonant energies of the random and quasiperiodic systems.

On the other hand, the numerical studies of wavefunctions show that some wavefunctions at specific energies of 1D disorder and quasiperiodic systems behave much like the conventional Bloch states. In particular, we note that the envelopes of some calculated wavefunctions for some totally different lattices have exactly the same features. In this paper, we will try to reveal the relationship of these characteristic wavefunctions with the 1D perfect periodic systems and suggest that the envelopes of these wavefunctions can be generally used as a criterion of the delocalization-localization transition of the electronic states in the random and quasiperiodic lattices.

The outline of the paper is as follows. In Sec. 2 we obtain a analytical expression from which the resonant energies of the random and quasiperiodic systems with the symmetric defects can be easily determined. In Sec. 3, we show that for the periodic lattice the simplest wavefunctions can be observed at some special energies. Then, by using the expression of Sec. 2, we derive the resonant energies for some quasiperiodic and random systems and perform numerical simulations of the spatial distribution for the electronic states near the obtained resonant energies. Finally, a brief summary is given in Sec. 4.

## 2. Resonant Energies

In the tight-binding and nearest-neighbor interaction approximation, the equation of motion is given by

$$(E - \varepsilon_i)c_i - t_{i+1}c_{i+1} - t_i c_{i-1} = 0\,, \tag{1}$$

where $c_i$ and $c_{i\pm1}$ are the site amplitudes, $\varepsilon_i$ is the site energy, $t_i$ and $t_{i+1}$ are the nearest-neighbor matrix elements. Equation (1) can be rewritten in the matrix form

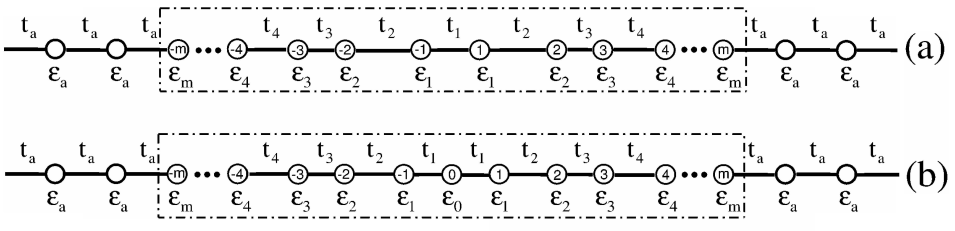


Fig. 1. (a) A symmetric defect with even atoms; (b) a symmetric defect with odd atoms.

$$\begin{bmatrix} c_{i+1} \\ c_i \end{bmatrix} = P_i \begin{bmatrix} c_i \\ c_{i-1} \end{bmatrix}, \tag{2}$$

and

$$P_i = \begin{bmatrix} \dfrac{E-\varepsilon_i}{t_{i+1}} & -\dfrac{t_i}{t_{i+1}} \\ 1 & 0 \end{bmatrix}, \tag{3}$$

where $P_i$ is the promotion matrix which connects the adjacent site amplitudes $c_i$ and $c_{i\pm1}$.

From Eqs. (2) and (3), the relation of the site amplitudes which connects both ends of a $N$-atom defect is

$$\begin{bmatrix} c_{n+N+1} \\ c_{n+N} \end{bmatrix} = \underline{P} \begin{bmatrix} c_{n+1} \\ c_n \end{bmatrix}, \tag{4}$$

where $\underline{P}$ is the total transfer matrix which is given by $\underline{P} = P_{n+N+1}P_{n+N}\cdots P_{n+2}P_{n+1}$.

In this work, we will restrict our investigation to the defects having the SIS. There are many kinds of defects with the SIS. It is noted that these defects can be generally divided into two classes. The first class consists of even atoms (see Fig. 1(a)), while the second, as shown in Fig. 1(b), has odd atoms among a defect. We now proceed with the derivation of the expression of the resonant energies for these two defects.

Let us consider, firstly, the defect of Fig. 1(a), where the atoms are embedded at site $-m,\ldots,-1,1,\ldots,m$ in a 1D periodic lattice. Using Eqs. (2) and (3), we write the total transfer matrix across the defect as

$$\underline{P} = P_{-m}\cdots P_{-i}\cdots P_{-2}P_{-1}P_1P_2\cdots P_i\cdots P_m\,. \tag{5}$$

From the definition of Eq. (3), we get an interesting relationship among the matrices:

$$P_{-i} = \begin{bmatrix} \dfrac{E-\varepsilon_i}{t_i} & -\dfrac{t_{i+1}}{t_i} \\ 1 & 0 \end{bmatrix} = SP_i^{-1}S^{-1}\,, \tag{6}$$

where $S = \begin{bmatrix} 0 & 1 \\ 1 & 0 \end{bmatrix}$.

For convenience, Eq. (5) can be rewritten in the following form:

$$\underline{P} = P_L \cdot P_R \,. \tag{7}$$

By using Eqs. (5) and (6), we obtain

$$P_R = P_1 P_2 P_3 \cdots P_i \cdots P_m = \begin{bmatrix} a & b \\ c & d \end{bmatrix}, \tag{8}$$

$$P_L = P_{-m} \cdots P_{-i} \cdots P_{-3} P_{-2} P_{-1} = S P_R^{-1} S^{-1} \,, \tag{9}$$

where $a, b, c$ and $d$ are the four elements of the matrix $P_R$. By substituting Eqs. (8) and (9) into Eq. (7), after some algebra we get

$$\underline{P} = \begin{bmatrix} \dfrac{b^2 - a^2}{bc - ad} & -\dfrac{bd - ac}{bc - ad} \\ \dfrac{bd - ac}{bc - ad} & \dfrac{c^2 - d^2}{bc - ad} \end{bmatrix}. \tag{10}$$

Similarly, for the symmetry defect of Fig. 1(b), the total transfer matrix can be expressed as

$$\underline{P} = P_L P_0 P_R \,, \tag{11}$$

where $P_L$ and $P_R$ are given by Eqs. (8) and (9), respectively. The transfer matrix $P_0$ for this defect is given by

$$P_0 = \begin{bmatrix} \dfrac{E - \varepsilon_0}{t_1} & -1 \\ 1 & 0 \end{bmatrix} = \begin{bmatrix} f & -1 \\ 1 & 0 \end{bmatrix}.$$

Then the total transfer matrix of Eq. (11) can be written as

$$\underline{P} = \begin{bmatrix} \dfrac{b(2a + bf)}{bc - ad} & -\dfrac{ad + bc + bdf}{bc - ad} \\ \dfrac{ad + bc + bdf}{bc - ad} & -\dfrac{d(2c + df)}{bc - ad} \end{bmatrix}. \tag{12}$$

It follows directly from Eqs. (10) and (12) that, for both cases, the total transfer matrix can be represented by a $2 \times 2$ antisymmetric matrix

$$\underline{P} = \begin{bmatrix} A & -B \\ B & C \end{bmatrix}. \tag{13}$$

To study the problem of transmission properties through a defect which is characterized by the total transfer matrix $\underline{P}$, we can suppose the defect is placed at site

$n+1$ to $N+n+1$ in an otherwise perfect lattice. Then, we have the site amplitudes to both sides of the defect as

$$c_j = \begin{cases} e^{ikj} + re^{-ikj} & \text{for } j \leq n+1\,, \\ te^{ikj} & \text{for } j \geq n+N+1\,. \end{cases} \tag{14}$$

Generally, for the given $\underline{P}$ and $k$ of Eq. (14), Wu *et al.*[19] have found the reflection amplitude $r$:

$$r = -Z^{2N} \frac{\alpha^T \Gamma \underline{P} \alpha}{\alpha^T \Gamma \underline{P} \alpha^*}\,, \tag{15}$$

where

$$Z = e^{ik}, \qquad \Gamma = \begin{bmatrix} 0 & 1 \\ -1 & 0 \end{bmatrix}, \qquad \alpha = \begin{bmatrix} Z \\ 1 \end{bmatrix},$$

and $\alpha^T$ is the transpose of $\alpha$.

From Eq. (15), Wu *et al.*[19] have pointed out that the reflection coefficient will vanish only when the matrix $\underline{P}$ is proportional to (i) the unit matrix or (ii) the promotion matrix for the ordered system (or some linear combination of both). Namely, when the defect is inserted into a tight-binding monatomic chain, for which the site energy is $\varepsilon_a$ and atoms connected by the same hopping interaction $t_a$. The transparency condition ($r = 0$) can be explicitly expressed as

$$\underline{P} = \xi \begin{bmatrix} \dfrac{E-\varepsilon_a}{t_a} & -1 \\ 1 & 0 \end{bmatrix} + \eta \begin{bmatrix} 1 & 0 \\ 0 & 1 \end{bmatrix}, \tag{16}$$

where $\xi$ and $\eta$ are the constants.

In fact, Eq. (16) implies that the reflection coefficient of the system will vanish only when the total transfer matrix of the defect is a $2 \times 2$ antisymmetric matrix. Surprisingly, our analytical results of Eqs. (10) and (12) indicate clearly that the transparency condition of Eq. (16) can necessarily be met when internal structure is built into the defects. Consequently, it is clear that at some values of $E$, Eq. (16) will be satisfied for any defects having SIS. In the light of the above results, a general expression for determining the resonant energies of 1D systems with any kind of symmetric defects can be expressed in a straight-forward manner as

$$A - \frac{B(E-\varepsilon_a)}{t_a} - C = 0\,. \tag{17}$$

Note that the transfer matrix of Eq. (13) is unimodular, and hence we arrive at the condition

$$AC + B^2 = 1. \tag{18}$$

From Eqs. (17) and (18), it is evident that the resonant energies of the systems with the defects having the SIS are related only to the host parameters $\varepsilon_a$, $t_a$ and two matrix elements of the total transfer matrices of the defects. We should point

out that all our analytical results given in the next section are obtained directly from Eq. (17).

## 3. Wavefunctions

### 3.1. *Characteristic wavefunctions of 1D periodic system*

It is known that the energy spectrum in 1D quasiperiodic systems is a Cantor set and the wavefunctions are either self-similar or chaotic.[34–36] However, recent studies of the wavefunctions in these systems show that there exist some energies for which the wavefunctions behave like the Bloch states. To our astonishment, similar wavefunctions have been seen even in some random systems. These findings imply the possible connection between the Bloch-like extended states of non-periodic systems and perfect periodic lattices (PPL).

Now, let us turn our attention to the spatial distributions of the wavefunctions of the one-dimensional PPL. For the PPL with the site energy $\varepsilon_a$ and the hopping interaction $t_a$, the whole energy band of this lattice ranges from $[E_L, E_R] = [-2t_a + \varepsilon_a, 2t_a + \varepsilon_a]$ and the eigenstates are simple Bloch states of the form $e^{ikn}$. Despite these obvious results, there is a simple but interesting question:

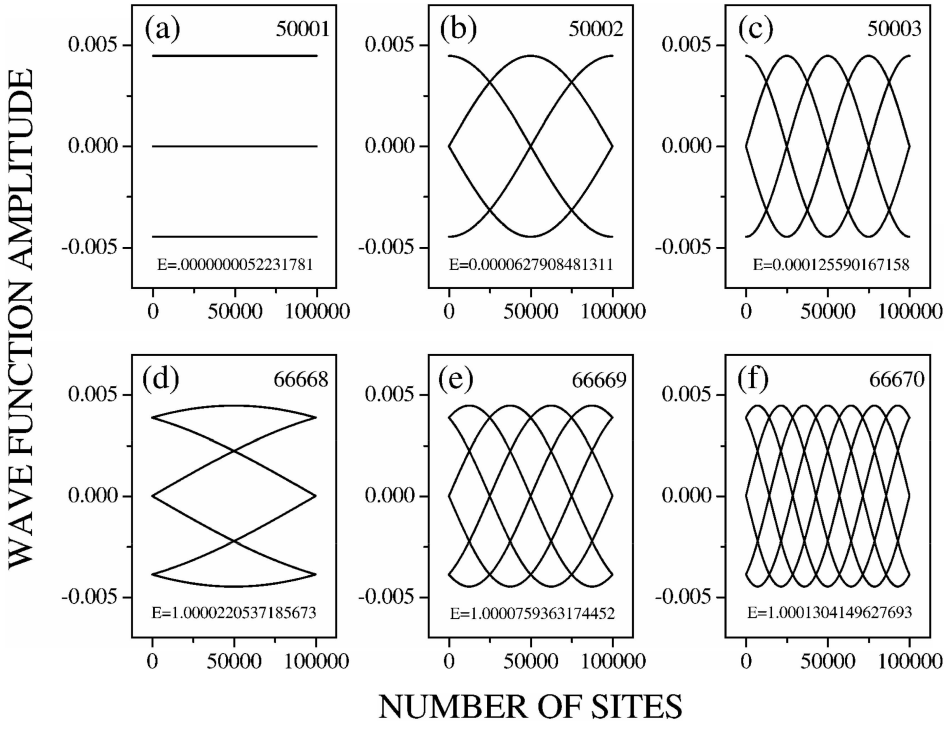


Fig. 2. Example of six states in the one-dimensional perfect periodic lattice. (a)–(c) and (d)–(f) for the eigenenergies nearest to the special values of 0.0 and 1.0, respectively.

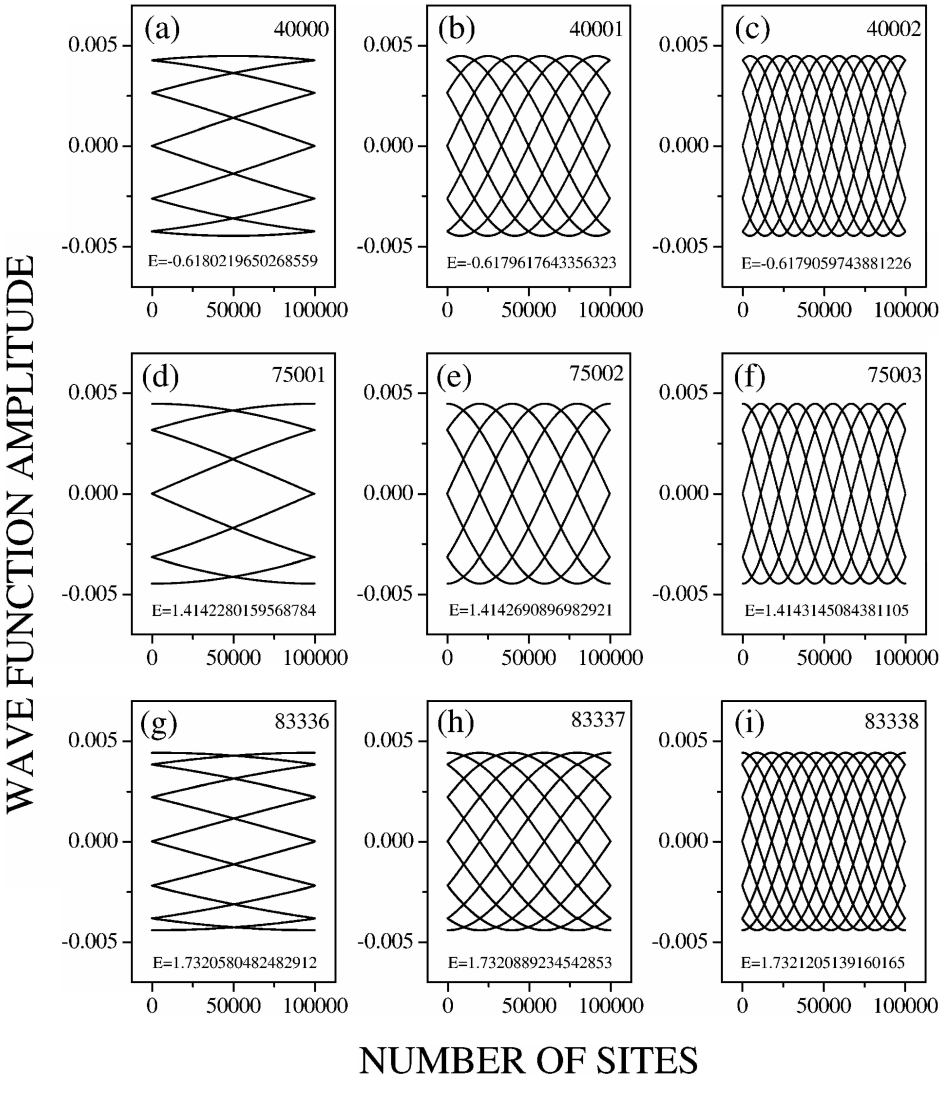


Fig. 3. Example of nine states in the one-dimensional perfect periodic lattice. (a)–(c), (d)–(f) and (g)–(i) for the eigenenergies nearest to the special values of $-\tau$, $\sqrt{2}$, and $\sqrt{3}$, respectively.

What kind of specific pattern of the wavefunctions can be observed for these Bloch states? However, much less attention has been paid to the study of this question. Here, we calculate the wavefunctions for the on-site version of this lattice.

For the given parameters ($\varepsilon_a = 0$, $t_a = 1$), the energy band of the PPL is $[-2, 2]$. We have numerically calculated the wavefunctions for energies ranging over the whole spectrum and found that the simplest spatial structures of the eigenfunctions exist only around some special energy values: (a) the eigenvalues are integer, they are $0, \pm 1, \pm 2$; (b) the eigenvalues are irrational, they are $\pm\tau$, $\pm(1+\tau)$, $\pm\sqrt{2}$,

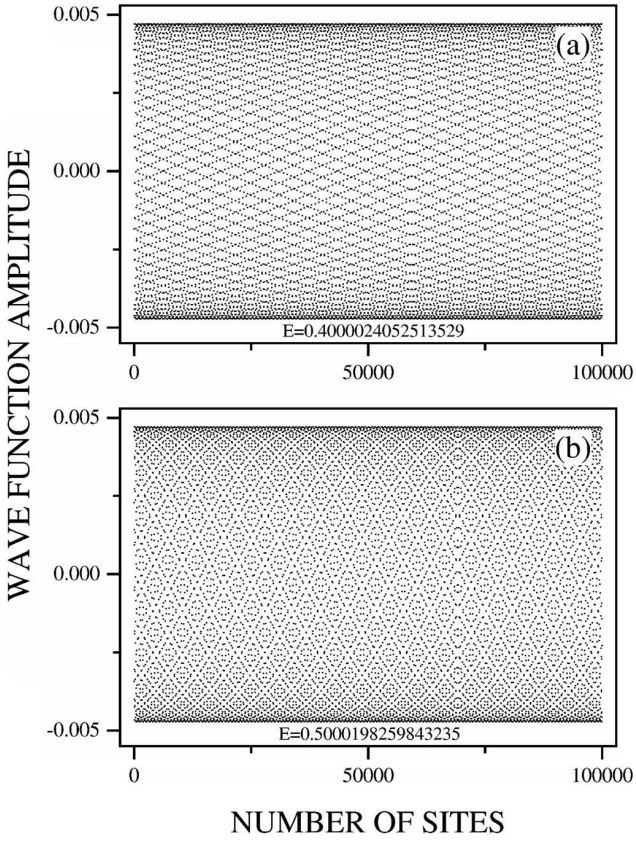


Fig. 4. Two complicated wavefunctions of the one-dimensional perfect periodic lattice. The corresponding eigenenergies are far from the specific energies.

$\pm\sqrt{3}$, where $\tau = (\sqrt{5}-1)/2$. Examples of the wavefunctions are presented in Figs. 2 and 3 for cases (a) and (b), respectively. In the calculations, we have chosen the system consisting of 100,000 atoms. Figures 2(a)–(c) and 2(d)–(f) show the electronic wavefunctions with eigenvalues nearest to the special values 0.0 and 1.0, respectively. It should be noted that the extended state shown in Fig. 2 is periodic. The periodic difference between two nearest states is 3. Figures 3(a)–(c), 3(d)–(f), and 3(g)–(i) show the electronic wavefunctions with eigenvalues nearest to $-\tau$, $\sqrt{2}$ and $\sqrt{3}$, respectively. Here, the periodic difference between two nearest states is 4. We have investigated the properties of the wavefunction's envelopes for the PPL with totally different sites and found that the corresponding envelopes are exactly the same for the electronic states around the above special energies. Meanwhile, we find that the wavefunctions with the eigenenergies different from these special energies are much more complicated, examples of which are presented in Figs. 4(a) and (b).

In the following sections, we show that these findings (Figs. 2 and 3) can be

applied as a criterion of delocalization of the electronic states in 1D quasiperiodic and random lattices. In other words, in a 1D random or quasiperiodic system, if the delocalization electronic states are analytically predicted, then we can chose the system parameters and let the resonant energies be one of the above special energies. By calculating the wavefunctions of the corresponding eigenenergies, we can judge whether the electronic delocalization-localization transition indeed occurs around the studied energy.

### 3.2. *Resonant energies and wavefunctions of quasiperiodic systems*

The one-dimensional generalized Fibonacci sequence is described by successive application of the substitution rules $A \to AB^n$ and $B \to A$, with $n$ being a positive integer, which is denoted as $GF(n)$ here. In these systems, the extended states have been found previously at individual energies.[6,7] Using real-space renormalization-group arguments, Sil *et al.*[8] have analytically shown that there is an infinite number of extended states in the transfer version of the $GF(2)$ chain. In this section, we will generalize and extend these studies. We would like to point out that similar extended wavefunctions to Figs. 2 and 3 can be easily found in many 1D quasiperiodic systems.

#### 3.2.1. *Transfer model of* $GF(2)$

First, we consider the transfer model of the quasiperiodic $GF(2)$ chain of Fig. 5(a). By inspecting this figure, we see that three atoms (marked by 1, 2 and 3 in the chain) always form a symmetry triplet defect in the lattice. Using Eq. (3), the transfer matrices for these sites can be expressed by

$$P_1 = \begin{bmatrix} \dfrac{E-\varepsilon_0}{t_b} & \dfrac{-t_a}{t_b} \\ 1 & 0 \end{bmatrix},$$

$$P_2 = \begin{bmatrix} \dfrac{E-\varepsilon_0}{t_b} & -1 \\ 1 & 0 \end{bmatrix}, \tag{19}$$

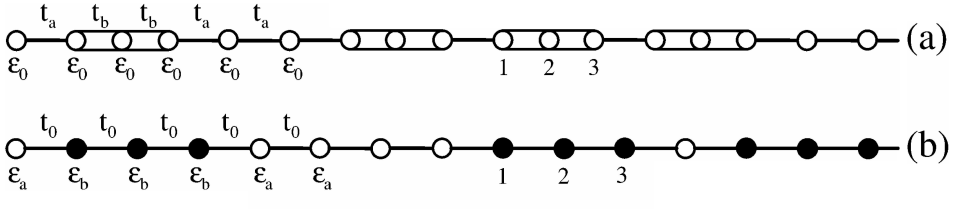


Fig. 5. (a) The transfer version of quasiperiodic $GF(2)$ lattice; (b) the on-site version of the quasiperiodic $GF(3)$ lattice.

$$P_3 = \begin{bmatrix} \dfrac{E-\varepsilon_0}{t_a} & \dfrac{-t_b}{t_a} \\ 1 & 0 \end{bmatrix}.$$

Then the total promotion matrix $\underline{P}$ is

$$\begin{aligned} \underline{P} &= P_3 P_2 P_1 \\ &= \begin{bmatrix} \dfrac{(E-\varepsilon_0)^3 - 2t_b^2(E-\varepsilon_0)}{t_a} & 1 - \left(\dfrac{E-\varepsilon_0}{t_b}\right)^2 \\ \left(\dfrac{E-\varepsilon_0}{t_b}\right)^2 - 1 & \dfrac{-t_a(E-\varepsilon_0)}{t_b^2} \end{bmatrix}. \end{aligned} \tag{20}$$

From Eq. (17), one obtains

$$(E-\varepsilon_0)\left(\frac{t_a^2 - t_b^2}{t_a t_b^2}\right) = 0\,, \tag{21}$$

and the resonant energy

$$E = \varepsilon_0\,.$$

We now present some results of our calculations for this resonant energy, taking the parameters as $\varepsilon_0 = 0$, $t_a = 1$ and $t_b = 2$, which have been used in Ref. 6. Figures 6(a)–(c) show the first three eigenenergies around $E = \varepsilon_0$. In fact, Fig. 6(a) have been numerically and theoretically reported.[8] It is of special interest to compare these figures with Figs. 2(a)–(c) of the periodic systems. It seems as if these figures are constructed by the superposing of two corresponding wavefunctions of Fig. 2 of different amplitudes. Let us denote the amplitudes for these sub-wavefunctions by $|A_L|$ and$|A_S|$, respectively. We find $|A_L| / |A_S| = |t_b/t_a|$.

### 3.2.2. *On-site model of GF*(3)

Figure 4(b) is the on-site model of $GF(3)$. By analogy with Ref. 6, the parameters are chosen as: $\varepsilon_a = 1, \varepsilon_b = -1$, and $t_a = -1$. The trimer-like defects can be found in the lattice, some of which are indicated by 1, 2 and 3 in Fig. 4(b). From the transfer matrices of the defect and some algebraic manipulation, we obtain the total transfer matrix:

$$\underline{P} = \begin{bmatrix} 2(E+\varepsilon_a) - (E+\varepsilon_a)^3 & 1 - (E+\varepsilon_a)^2 \\ (E+\varepsilon_a)^2 - 1 & E+\varepsilon_a \end{bmatrix}. \tag{22}$$

The resonant energies are now determined by the following expression:

$$-\varepsilon_a \left[(E+\varepsilon_a)^2 - 1\right] = 0\,. \tag{23}$$

Then, two resonant energies are

$$E_1 = 1 - \varepsilon_a \quad \text{and} \quad E_2 = -1 - \varepsilon_a\,.$$

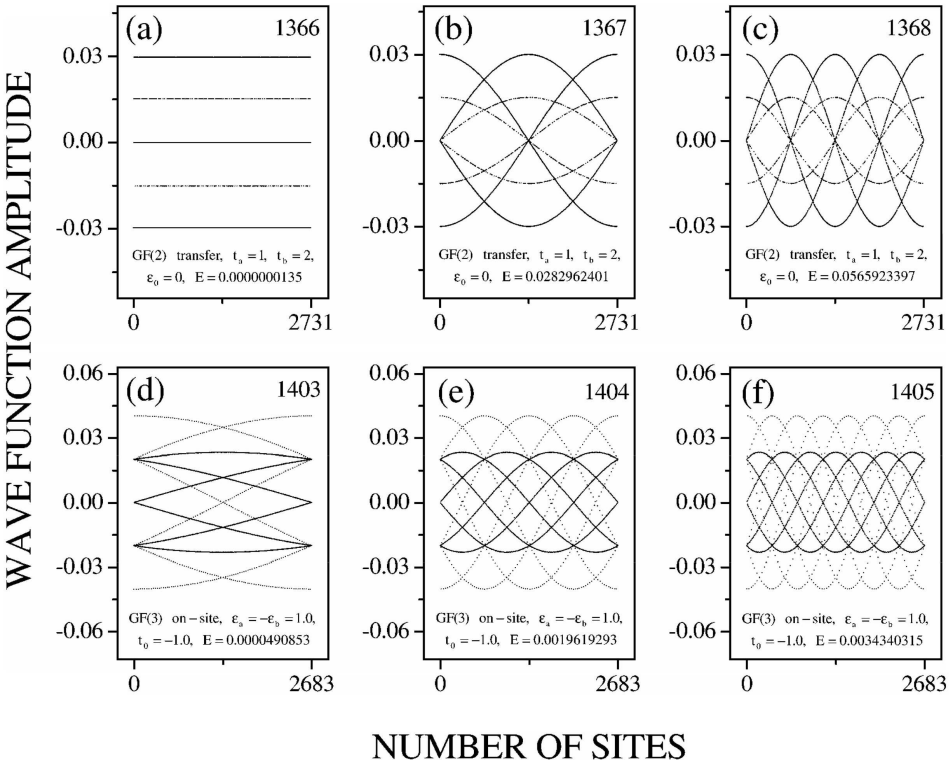


Fig. 6. (a)–(c) Examples of three wavefunctions in the one-dimensional transfer model of $GF(2)$; the corresponding eigenenergies are nearest to the specific energy $E = 0.0$ of the perfect periodic lattice. (d)–(f) Examples of three wavefunctions in the one-dimensional on-site model of $GF(3)$; the corresponding eigenenergies are nearest to the specific energy $E = 1.0$ of the perfect periodic lattice.

Since $E - \varepsilon_a = 2t_a \cos k$, for the given $\varepsilon_a$ and $t_a$, the corresponding energy band is $[-1, 3]$. Consequently, only one resonant energy $E_1 = 1 - \varepsilon_a = 0.0$ remains. This resonant energy corresponds to $E = 1.0$ of the same system with $\varepsilon_a = 0.0$. Therefore, similar wavefunctions to Figs. 2(d)–(f) can be expected in this system when the eigenenergies are near to $E_1 = 0.0$. Figures 6(d)–(f) show the wavefunctions of first three eigenenergies around $E_1$, among which only a single state of Fig. 6(f) has been reported.[6] It is of special interest to note that the wavefunctions are also composed of two sub-wavefunctions in these figures. The one with the bold scatter graph and small amplitudes resembles the corresponding figures of Fig. 2(d)–(f), while the one with the thin scatter graph and large amplitudes is similar to Figs. 2(b)–(c) of the periodic system. In any case, the characteristic structures of Figs. 2(d)–(f) of the PPL can be clearly seen in these figures. We also find the amplitudes of these two sub-wavefunctions satisfy $|A_{\text{bold}}/A_{\text{thin}}| = \tau \simeq 0.6180339887$.

It would be interesting to extend these studies in the future in order to consider how the long-range interactions rather than the short-range interactions influence the properties of wavefunctions in the quasiperiodic systems.

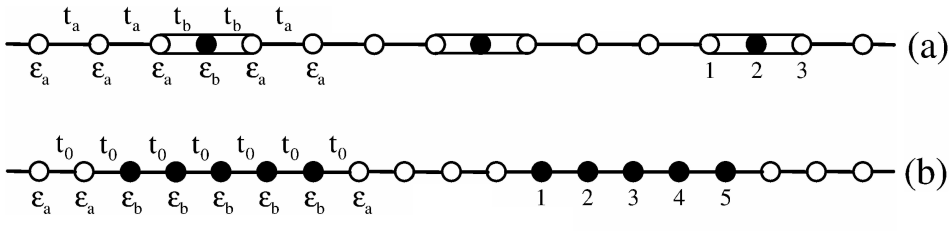


Fig. 7. (a) Defects in the repulsive binary alloy; (b) 5-mer defects in the random five-mer model.

### 3.3. *Resonant energies and wavefunctions of random systems*

Thus far, we have shown theoretically the resonant energies of the quasiperiodic systems and performed a great number of numerical calculation of the eigenfunctions. In what follow, we will turn to study the random systems of Fig. 7. These two models were proposed by Wu Goff and Phillips,[19] and relatively little work has been done on these systems. Similarly, by using the formula (17), we derive the resonant energies of the studied systems, then the numerical results of the corresponding eigenfunctions.

#### 3.3.1. *Repulsive binary alloy defect*

Figure 7(a) shows the repulsive binary alloy (RBA), and the triplet defect "123" possesses symmetric internal structure. The total transfer matrix across the defect is obtained as

$$\underline{P} = \begin{bmatrix} D & 1 - \dfrac{(E-\varepsilon_a)(E-\varepsilon_b)}{t_b^2} \\ \dfrac{(E-\varepsilon_a)(E-\varepsilon_b)}{t_b^2} - 1 & \dfrac{-t_a(E-\varepsilon_b)}{t_b^2} \end{bmatrix}, \tag{24}$$

where $D = (E+\varepsilon_a)(E^2 + \varepsilon_a\varepsilon_b - E\varepsilon_a - E\varepsilon_b - 2t_b^2)/t_a t_b^2$.

In this case, Eq. (17) can be written as

$$E\left(\frac{t_a^2 - t_b^2}{t_a t_b^2}\right) + \frac{\varepsilon_a t_b^2 - \varepsilon_b t_a^2}{t_a t_b^2} = 0\,. \tag{25}$$

Then, the expression for the resonant energy is[19]

$$E = \frac{\varepsilon_b t_a^2 - \varepsilon_a t_b^2}{t_a^2 - t_b^2}\,. \tag{26}$$

We calculate the wavefunctions of this state for two cases. In each case, we take the size of system $N = 2{,}000$, and the parameters $\varepsilon_a = 0.0$ and $t_a = 1.0$. Figures 8(a) and (b) show the wavefunctions for the system with parameters $\varepsilon_b = -1$, $t_b = \sqrt{2}$ and $\varepsilon_b = 1$, $t_b = \tau$, respectively. The main envelopes of these two wavefunctions are the same as Figs. 2(f) and 3(f) of the periodic system. These represent the solid evidence of delocalization of the electronic states in the RBA.

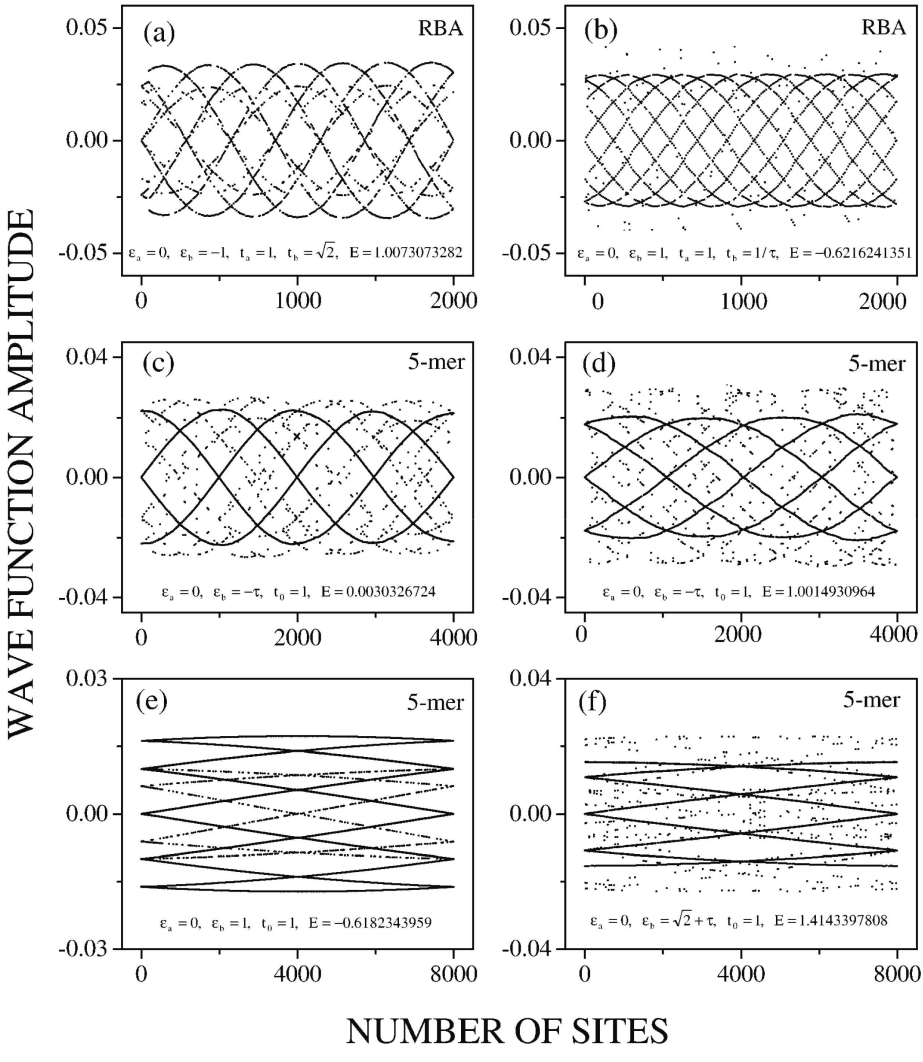


Fig. 8. (a)–(b) Examples of two wavefunctions in the one-dimensional repulsive binary alloy; the corresponding eigenenergies are nearest to the specific energies $E = 1.0$ and $E = -\tau$, respectively. (c)–(f) Examples of four wavefunctions in the one-dimensional random five-mer model; the corresponding eigenenergies are nearest to the specific energies $E = 0.0$, $E = 1.0$, $E = -\tau$, and $E = \sqrt{2}$, respectively.

### 3.3.2. *Random five-mer defect*

In the random five-mer model (shown in Fig. 7(b)), the atoms among a defect can be labeled as 1, 2, 3, 4 and 5. Consequently, we can get five individual transfer matrixes from Eq. (3) and the total transfer matrix from Eq. (11). The expression for the resonant energies is

$$E^4 - 4\varepsilon_b E^3 + (6\varepsilon_b^2 - 3)E^2 + (6\varepsilon_b - 4\varepsilon_b^3)E + 1 - 3\varepsilon_b^2 = 0\,, \tag{27}$$

and the four resonant energies are

$$\begin{aligned} E_1 &= \varepsilon_b - \tau, \qquad & E_2 &= \varepsilon_b + \tau\,, \\ E_3 &= \varepsilon_b - (1+\tau), \qquad & E_4 &= \varepsilon_b + (1+\tau)\,. \end{aligned} \tag{28}$$

Equation (28) is obtained under one set of special parameters, $\varepsilon_a = 0.0$ and $t_a = 1.0$. Because $E_i$ $(i = 1, 2, 3, 4)$ must be the energy of the ordered band, they are limited by the equation $E_i = 2\cos k$. Consequently, for the given parameters, only some of the resonant energies are allowed in the studied system. We obtain the following allowed resonant energies and corresponding conditions:

$$\begin{cases} E_1, E_2, E_3, E_4, & \text{if } \tau - 1 \le \varepsilon_b \le 1 - \tau\,, \\ \begin{cases} E_1, E_2, E_3, & \text{if } \ 1 - \tau < \varepsilon_b \le 2 - \tau\,, \\ E_1, E_2, E_4, & \text{if } \ \tau - 2 \le \varepsilon_b < \tau - 1\,, \end{cases} \\ \begin{cases} E_1, E_3, & \text{if } \ 2 - \tau < \varepsilon_b \le 2 + \tau\,, \\ E_2, E_4, & \text{if } \ -2 - \tau \le \varepsilon_b < \tau - 2\,, \end{cases} \\ \begin{cases} E_3, & \text{if } \ 2 + \tau < \varepsilon_b \le 3 + \tau\,, \\ E_4, & \text{if } \ -3 - \tau \le \varepsilon_b < -2 - \tau\,. \end{cases} \end{cases} \tag{29}$$

Now, we will calculate the wavefunctions of the above resonant energies for several cases of the random 5-mer system: (i) When $\varepsilon_b = -\tau$ , then $E_1 = -2\tau$, $E_2 = 0.0$, and $E_4 = 1.0$ are allowed. Figures 8(c) and (d) show two wavefunctions for the eigenenergies near to $E_2 = 0.0$ and $E_4 = 1.0$, respectively. As seen in these figures, the bold scatter graphs are identical to Figs. 2(c) and (e) of the PPL. (ii) When $\varepsilon_b = 1.0$, from Eq. (29), the possible resonant energies are $E_1 = 1 - \tau$, $E_2 = 1 + \tau$, and $E_3 = -\tau$; for this case, we calculate the wavefunction of the eigenenergy which is nearest to $E_3 = -\tau$, and the wavefunction similar to Fig. 3(a) is shown in Fig. 8(e). Finally, (iii) we chose $\varepsilon_b = \sqrt{2} + \tau$, and consequently, only $E_1 = \sqrt{2}$, $E_3 = \sqrt{2} - 1$ remain. Figure 8(f) is the wavefunction for the electronic state of the system with the energy value nearest to the special energy $E_1 = \sqrt{2}$. Clearly, this figure is similar to Fig. 3(d) for the periodic system. Here we wish to point out that during the numerical calculations we have by design chosen the studied systems with various sites.

By selecting some appropriate parameters, the wavefunctions such as Figs. 3(g)–(i) of the special energy $\sqrt{3}$ can also be found in these systems. Our numerical simulations here agree very well with theoretical predications. With these interesting results, it will be no surprise to find the Bloch-like electronic states in quasiperiodic and random systems.

## 4. Summary

In this work we have studied the relationship between the resonant energies and the wavefunctions in one-dimensional (1D) quasiperiodic and random systems. First, we

have shown that, for any one-dimensional systems with the symmetric defect, the corresponding total transfer matrix is a $2 \times 2$ antisymmetric matrix. This is quite a remarkable result, which is consistent with the criteria suggested by Wu, Goff and Phillips. Then we have obtained analytically the expression which has been proved to be powerful in determining the resonant energies of 1D quasiperiodic and random systems. Second, we have found some interesting wavefunction structures at some specific energies of the 1D perfect periodic lattice and suggested that the envelopes of these wavefunctions can be widely applied as the criterion of delocalization of the electronic states in the studied systems. Further numerical results indicate that Bloch-like electronic states can easily be found in some non-periodic systems. There is no doubt that the method developed in this paper can be expected to have many applications in the investigation of the delocalization properties of 1D quasiperiodic and random systems.

## Acknowledgments

This work was supported by grants from National Nature Science Foundation of China, and the State Key Program for Basic Research from the Ministry of Science and Technology of China, NSF of Jiangsu and partly by the Ministry of Education of China and Fok Ying Tung Education Foundation.

## References

1. V. Kumar and G. Ananthakrishna, *Phys. Rev. Lett.* **59**, 1476 (1987).
2. V. Kumar, *J. Phys. Condens. Matter* **2**, 1349 (1990).
3. E. Macia and F. Dominguez-Adame, *Phys. Rev. Lett.* **76**, 2957 (1996).
4. X. Q. Huang and C. D. Gong, *Phys. Rev.* **B58**, 739 (1998).
5. E. Macia, *Phys. Rev.* **B60**, 10032 (1999).
6. M. Severin and R. Riklund, *Phys. Rev.* **B39**, 10362 (1989).
7. J. Q. You, J. R. Yan, T. Xie, X. Zheng and J. X. Zhong, *J. Phys.: Condens. Matter* **3**, 7255 (1991).
8. S. Sil, S. N. Karmakar, R. K. Moitra and A. Chakrabarti, *Phys. Rev.* **B48**, 4192 (1993).
9. X. J. Fu, Y. Y. Liu, Z. Z. Guo, P. Q. Zhou and X. Q. Huang, *Phys. Rev.* **B51**, 3910 (1995).
10. R. Riklund, M. Severin and Y. Liu, *Int. J. Mod. Phys.* **B1**, 121 (1987).
11. A. Chakrabarti, S. N. Karmakar and R. K. Moitra, *Phys. Rev. Lett.* **74**, 1403 (1995).
12. S. Chattopadhyay and A. Chakrabarti, *Phys. Rev.* **B63**, 132201 (2001).
13. A. Ghost and S. N. Karmakar, *Phys. Rev.* **B61**, 1051 (2000).
14. R. Oviedo-Roa, L. A. Perez and C. Wang, *Phys. Rev.* **B62**, 13805 (2000).
15. D. H. Dunlap, H.-L. Wu and P. Phillips, *Phys. Rev. Lett.* **65**, 88 (1990).
16. S. DasSarma, S. He and X. C. Xie, *Phys. Rev.* **B41**, 5544 (1990).
17. H.-L. Wu and P. Phillips, *Phys. Rev. Lett.* **66**, 1366 (1991).
18. P. Phillips and H.-L. Wu, *Science* **252**, 1805 (1991).
19. H. L. Wu, W. Goff and P. Phillips, *Phys. Rev.* **B45**, 1623 (1992).
20. J. C. Flores and M. Hilke, *J. Phys.* **A26**, L1255 (1993).
21. C. M. Soukoulis, M. J. Velgakis and E. N. Economou, *Phys. Rev.* **B50**, 5110 (1994).

22. F. C. Lavarda, M. C. dos Santos, D. S. Galvao and B. Laks, *Phys. Rev. Lett.* **73**, 1267 (1994).
23. A. Sánchez, F. Domínguez- Adame, G. Berman and F. Izailev, *Phys. Rev.* **B51**, 6769 (1995).
24. M. Hilke and J. C. Flores, *Phys. Rev.* **B55**, 10625 (1997).
25. X. Q. Huang, X. T. Wu and C. D. Gong, *Phys. Rev.* **B55**, 11018 (1997).
26. M. Hilke, J. C. Flores and F. Dominguez-Adame, *Phys. Rev.* **B58**, 8837 (1998).
27. X. Huang, *Phys. Rev.* **B60**, 12099 (1999).
28. W. J. Deng, *Physica* **B279**, 224 (2000).
29. E. Lazo and M. E. Onell, *Phys. Lett.* **A283**, 376 (2001).
30. X. Q. Huang, R. W. Peng, F. Qiu, S. S. Jiang and A. Hu, *Eur. Phys. J.* **B23**, 275 (2002).
31. Y. M. Liu, R. W. Peng, X. Q. Huang, M. Wang, A. Hu and S. S. Jiang, *Phys. Rev.* **B67**, 205209 (2003).
32. X. Q. Huang, S. S. Jiang, R. W. Peng and A. Hu, *Phys. Rev.* **B63**, 245104 (2001).
33. R. W. Peng, X. Q. Huang, M. Wang, A. Hu, S. S. Jiang and M. Mazzer, *Appl. Phys. Lett.* **80**, 3063 (2002).
34. M. Kohmoto, L. P. Kadanoff and C. Tang, *Phys. Rev. Lett.* **50**, 1870 (1983).
35. Y. Y. Liu and R. Riklund, *Phys. Rev.* **B35**, 6034 (1987).
36. X. C. Xie and S. Das Sarma, *Phys. Rev. Lett.* **60**, 1585 (1985).